Modeling and Simulation of a Pneumatically-Actuated Rescue Robot

Hannes G. Daepp and Wayne J. Book
Georgia Institute of Technology

ABSTRACT

A four-legged pneumatically actuated search and rescue robot is presented as a system with potentially enhanced versatility relative to existing rescue robots. The usage of fluid powered actuation, combined with tele-operation of the robot via an operator workstation, enables the twelve degree of freedom robot to better manipulate large objects. A simulation is developed to enable ease of design variation and implementation testing in difficult virtual terrains. The simulation consists of an actuator model, modeled in Simulink, which is interfaced with an open-source dynamic simulation. The simulation calculates the robot dynamics based on actuator inputs. Where previous research has focused on the development of simulation kinematics and simple actuator models, this paper discusses development of a friction model for improved fidelity of the simulator, as well as implementation and verification in the dynamic model. The balance between model performance and the level of realism required for system development is found and discussed.

INTRODUCTION

Rescue robots appear increasingly often on disaster sites, using innovative mobile technologies to provide search assistance, but they have yet to actually rescue anyone[1]. This fact is indicative of a general lack throughout industry of lightweight mobile systems capable of precisely manipulating large loads. Indeed, there are many fields that would benefit from the development of such a platform, from rescue robotics[2] and military field robotics to agriculture or construction systems able to move large loads in terrains that humans cannot easily access. Fluid power offers a promising solution, as evidenced by the Compact Rescue Robot (CRR), a testbed of the NSF Center for Compact and Efficient Fluid Power (CCEFP).

The CRR is a pneumatically actuated four-legged robot that is tele-operated by an operator located at a remote workstation. Pneumatic actuation enables a high strength/weight ratio, creating a system capable of manipulating significant loads while requiring significantly energy to operate than an equivalent electrically actuated version would for an equal time period. Additionally, the legged configuration provides a solution to the challenges of traversing various landscapes[3].

The system further enhances its effectiveness through the use of haptic and A/V feedback to the operator. Improved haptics has been shown to have a more substantial effect on proper operator tele-presence than the enhancement of its visual counterpart[4]. Haptics is also efficient, providing signals that concisely provide comprehensive, intuitive directional and magnitude related information through direct interaction with the user[5], resulting in less ambiguous feedback than auditory or visual warning signals.

The CRR simulation described below presents a comprehensive basis for the evaluation of fluid power in robotics. The simulation couples modeling of pneumatic actuation in Simulink with an open source dynamic model of the CRR and environment simulation. The simulation effectively provides a prototype of the physical hardware and allows researchers to view the effects of system designs, changes to the operator interface, and control techniques that have not previously been studied with relative ease. Past examination[6] of the pneumatic actuator simulation has pointed to the need for a more accurate understanding of force applied by the cylinder. Accordingly, this paper examines the effect of friction on the cylinder force output.

While many researchers have simply approximated friction with a viscous damping term[7,8], several advanced models have been developed that examine the behavior of two contacting surfaces on a more sophisticated level, examining the behavior of the contacts on a microscopic scale. Many of these models, such as LuGre and Stribeck, though popular, are of limited use due to inherent discontinuities. Alternative methods such as Dankowicz have been developed to provide accurate, continuous friction models for very small velocities[7]. Such precise models, however, are used at the cost of complex development, consisting of detailed measurements, analysis and computation on a material level and are unnecessary for human-scale systems such as the CRR, where accurate system behavior on a microscopic scale is generally superfluous. Instead, variations on viscous and Coulomb friction models have been developed[7] and the components derived empirically[8], as will be done here.

In the first part of this paper, the system configuration is discussed and the components are detailed. Second, a single platform actuator simulation is developed, implemented in Simulink, tested with several friction approximations, and validated on a physical testbed. This simulation is then integrated with a readily available

open source dynamics package for multi-platform, practical simulation of manipulation and environmental interaction. Challenges are discussed, and results of the overall implementation are shown and compared to the results from the intermediate single-platform simulations. Future plans are discussed and conclusions are drawn.

SYSTEM CONFIGURATION

The system consists of four primary components: A physical prototype, an xPC Target Computer loaded with the central control software, the operator interface, and the multi-platform robot simulation, consisting of an actuator model within the central control software and a separate dynamics library, SrLib. The computer running xPC Target real-time software is a 1.4 GHz computer in the compact PC104 form factor, sampling at 1 GHz, while the other workstations use a Windows operating system. The basic interaction of the four components is depicted in Figure 1. Communication is as follows:

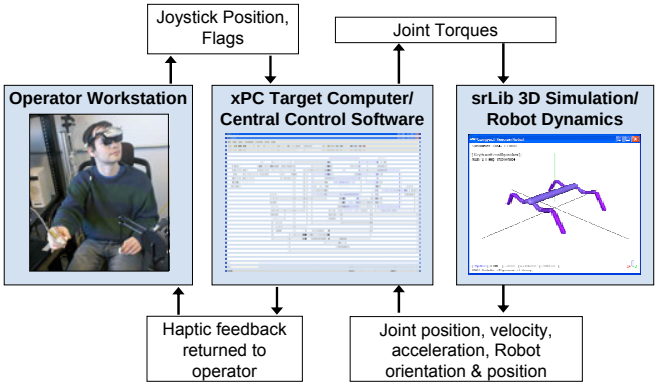

Figure 1 – System Configuration

1. Operator moves a Sensable Phantom™ haptic joystick on the operator workstation to command a motion of the robot end effector. The joystick position is sent via a wireless network through to the central control software on the xPC target.

2. The joystick end effector location is mapped to robot space and converted to joint angles using inverse kinematics. Each desired joint angle is sent to a PID controller that directs a voltage command to a pneumatic valve-cylinder model, which in turn sends a torque to the corresponding joint in SrLib.

3. SrLib uses the input torques, known model, and environment dynamics to generate position and velocity of each joint. These, in turn, are sent back to the xPC target.

4. Position and velocity data is supplied to the pneumatic actuator model and PID controller, and is converted to an end effector location using forward kinematics. This location is mapped to the Phantom joysticks and sent back to the operator interface via a wireless connection.

5. Position data is received by the operator workstation and used to provide haptic feedback to the operator through the Phantom joysticks.

For the case of the physical prototype, the voltage signal from the PID controller on the xPC target is routed directly to actuators on the prototype, which in turn sends back measured position and other sensory data. The components are discussed in detail below.

PHYSICAL ROBOT

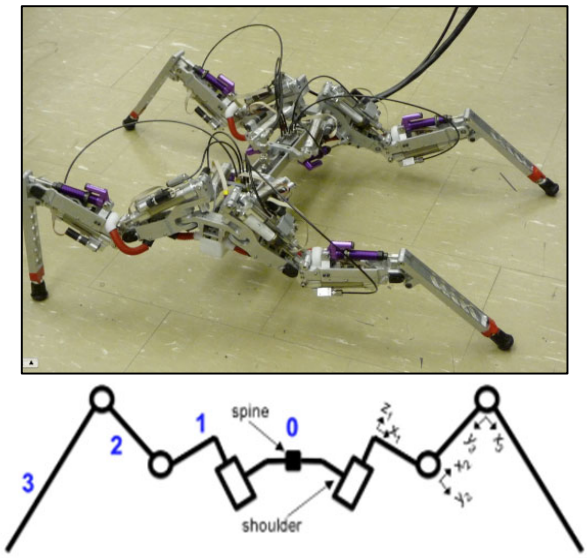

Figure 2 – *Top:* Physical Prototype of the Compact Rescue Crawler. *Bottom:* Diagram of robot kinematics as viewed from the front.

The robot (Figure 2) consists of a long spine with four 3-degree-of-freedom legs actuated by pneumatic cylinders. A physical model has been developed at Vanderbilt University and communicates with an xPC Target computer via a CANbus connection. A separate physical model consisting of two 3 degree-of-freedom legs attached to a fixed structure, communicates with an xPC target via UDP and is used as a platform for experimental manipulation and motion tests. Though the scale differs slightly between the two platforms, the kinematics of each leg are identical and are described by the Denavit-Hartenberg Parameters, shown in Table 1.

Table 1 – Denavit-Hartenberg Parameters (units in inches, degrees)

	θ	d	α	a
0	--	--	0	0
1	θ_1	1.608	-90	5.750
2	θ_2	0	0	6.828
3	θ_3	0	--	12.00
4	0	0	--	--

OPERATOR INTERFACE

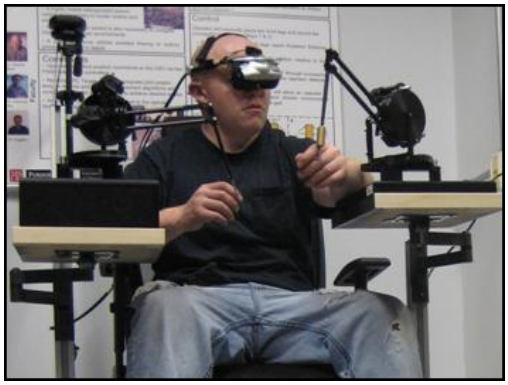

Figure 3 – Operator Workstation

The operator workstation (Figure 3) consists of two 3-degree of freedom Phantom™ haptic joysticks that the operator uses to control the robot. Audio-visual feedback from a pan-and-tilt camera on the robot is coupled with haptic feedback from the joysticks to provide the operator with a good sense of telepresence. Each joystick end effector corresponds to the end effector of one of the legs of the robot. When manipulating, this means that the operator can easily move the Phantom joysticks and observe equivalent motion of the front two legs of the robot. For gait motion in cases where user guidance is desired, a variant of a Follow-the-Leader gait[3] is used, in which the user places the front two legs, and the rear legs are placed automatically based on knowledge of the robot's balance and local environment.

DYNAMIC SIMULATION

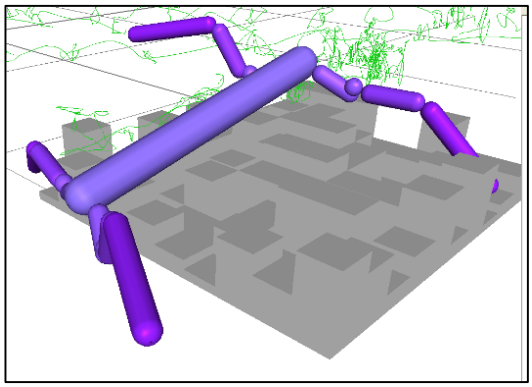

Figure 4 – Graphic Output from the SrLib Dynamic Simulation

The Seoul National University's Robotics Library (SrLib) was coupled with an actuator simulation, developed in Simulink and described below, to model the robot. SrLib is an open source library for multi-body dynamics and simulation in real-time, composed of simple rigid body shapes, joint types, actuation methods, and sensors. In addition to modeling the robot, the usage of SrLib also enabled easy modeling of sample terrains for studying environmental interaction. The output of SrLib is a visual rendering (Figure 4), as well as joint and link information such as position, velocity, and acceleration that is communicated back to the central control software on the xPC target via UDP communication.

PNEUMATIC ACTUATOR MODEL

The actuator model consists of a proportional directional control valve and a pneumatic cylinder. Voltage, position, and velocity of the cylinder piston are provided as inputs and applied force is output. This force is applied to the simple system models in the single-platform simulations performed in Simulink, and converted to a torque and sent to SrLib for the multi-platform actuator simulation.

The model is an extension of one that was discussed in a previous publication[6]. Whereas the previous model used a simple velocity dependent term to approximate friction, this paper analyzes practical friction modeling in detail. The term is broken into components that are determined using a physical cylinder model. Several friction models are then constructed and verified against a physical setup to choose the best level of accuracy while maintaining practicality in simulation.

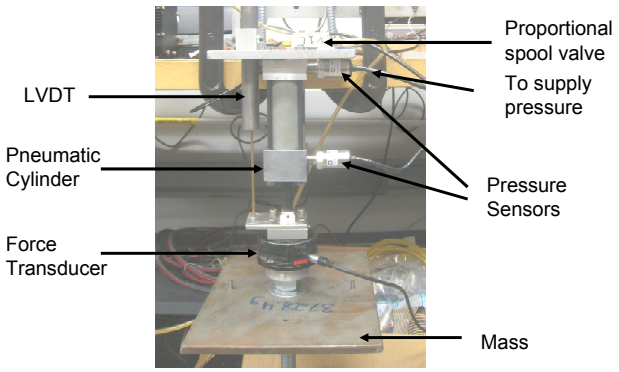

Figure 5 – Test setup for pneumatic actuator model validation

Experimental data used for model validation and friction analysis was collected using the test setup shown in Figure 5. The setup allows the user to send a voltage signal to a Festo MPYE-5-M5 proportional directional control valve using a PC104 running xPC Target / Simulink. The valve is connected to a custom 1.5-inch bore cylinder with a 1.5-inch stroke, mounted vertically in the Figure 5, though a horizontal orientation was also tested to ensure consistency with and without gravity contributions. A force sensor and LVDT were connected to the clevis of the piston to provide force and position feedback, respectively, while pressure sensors supply the user with the rod and cap pressure data for the cylinder. A threaded insert on the base of the force sensor allows the user to apply additional mass. The system was run at pressures ranging from 20 – 60 psi.

VALVE MODEL

The valve model accepts a 0-10 V input signal, applies discontinuities such as a saturation and dead zone, and is then multiplied by a gain corresponding to orifice area. A flag indicates whether supply or exhaust air is connected.

Several standardized variations of the mass flow rate equation have been defined. The approach used here, which is relatively common in literature, is based on the theoretical model of compressible flow through an orifice[10], shown in Equation 1. However, similar alternatives exist, such as that provided by the National Fluid Power Association (NFPA), which simplifies the calculation[11], or by the Instrument Society of America (ISA), which modifies the equation to account for internal valve flow geometry[10].

The mass flow can then be defined as a function of the discharge coefficient C_d, the orifice area A_0, the upstream and downstream pressures, P_u and P_d, and the corresponding upstream and downstream Temperatures, T_u and T_d, respectively. Temperature is calculated with the ideal gas law, using the instantaneous total mass and pressure in the cylinder, where R is the universal gas constant (287 J/kg K) and k is the ratio of specific heats (1.4).

$$\dot{m} = C_d A_0 f\left(P_u, T_u, P_d / P_u\right) \qquad (1)$$

Critical Pressure Ratio for air P_d / P_u =.528

If P_d / P_u > Critical (Un-Choked Flow):

$$f\left(P_u, T_u, P_u / P_d\right) = C_1 \frac{P_u}{\sqrt{T_u}} \left(\frac{P_d}{P_u}\right)^{1/k} \sqrt{1 - \left(\frac{P_d}{P_u}\right)^{(k-1)/k}} \qquad (2a)$$

$$C_1 = \sqrt{\frac{2k}{R(k-1)}}$$

If P_d / P_u ≤ Critical (Choked Flow):

$$f\left(P_u, T_u, P_u / P_d\right) = C_2 \frac{P_u}{\sqrt{T_u}} \qquad (2b)$$

$$C_2 = \sqrt{\frac{k}{R\left(\frac{k+1}{2}\right)^{(k+1)/(k-1)}}}$$

CYLINDER MODEL

A standard approach to modeling a pneumatic cylinder uses four states: x, $\dot{x}$, P_C, and P_R, representing stroke position, velocity, cap-side pressure, and rod-side pressure, respectively. The model is derived by inspecting each side of the cylinder independently and coupling the two sides into a single dynamics equation. A control volume is drawn about each side and an energy balance is written for that control volume based on the mass flow calculation and the volume change calculated by the dynamics equation and pressure equilibrium[8].

Cylinder Force Calculation

An energy balance, shown in Eq. (3), assumes the compressed gas obeys the ideal gas law and that the system is adiabatic—there is negligible heat transfer between the cylinder chambers and external atmosphere. This adiabatic assumption is generally acceptable for fast acting systems such as a walking robot.

$$\dot{P} = \frac{kRT\dot{m}}{xA} - \frac{P\dot{x}}{x}\left(\frac{kR}{c_p} + 1\right) \qquad (3)$$

The force applied by the cylinder to the system can then be shown to be a function of the cap-side and rod-side pressure and area, denoted respectively by subscripts c and r, as well as a friction term, discussed in detail below.

$$F_{cyl} = P_c A_c - P_r A_r - P_{atm} A_{piston} - F_{frict} \qquad (4)$$

Dynamics of the Physical System

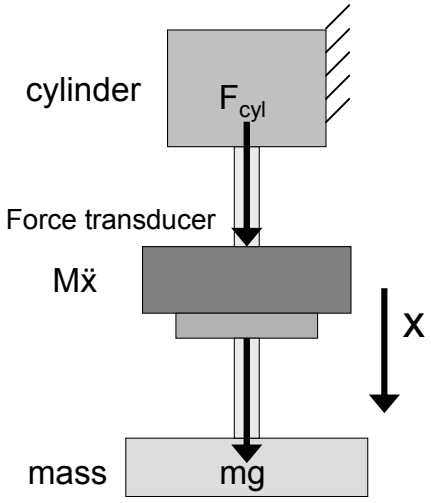

Figure 6 – Test Setup Configuration

In the multi-platform dynamic simulation described later in this paper, the force applied by the cylinder is converted to a torque and sent to the appropriate joint in SrLib. Within the model validation and friction analysis, however, a simpler system model is used, shown in the test setup to be a fixed, vertically oriented cylinder with a mass mounted at the base. This system, depicted in Figure 6, can be easily defined by equation 5, where M is the total mass of the piston and attached components:

$$M\ddot{x} = F_{cyl} + Mg \qquad (5)$$

The velocity and position outputs from this equation can then be sent back to the cylinder model for use in Equation 3.

FRICTION MODELING

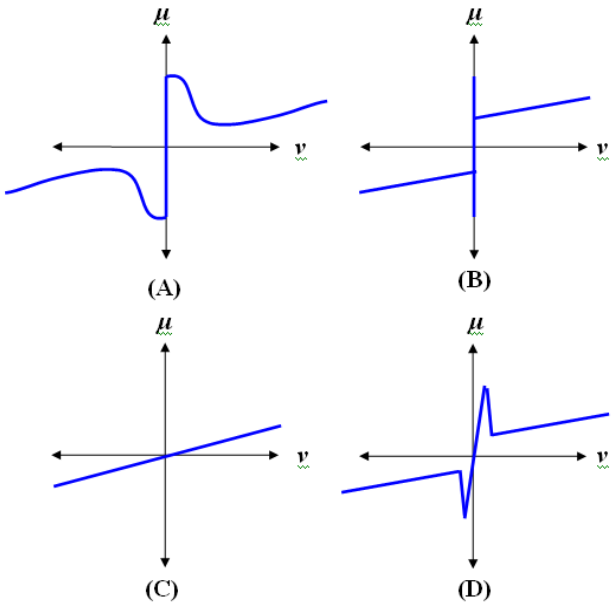

Figure 7 – General Forms for Friction Models Discussed Below (not to scale). (A) Stribeck Curve B) Discontinuous Coulomb-Viscous Friction (C) Viscous Friction (D) Continuous Coulomb-Viscous Friction

Friction plays an important role in cylinder output force calculation, particularly in low force or low velocity applications. Several popular friction models exist that are able to provide good friction approximations across a range of velocities, such as the LuGre and Stribeck Curves (Figure 7a). However, these models are difficult to implement practically because of the level of detail and comprehensive measurements necessary for their accurate calculation and because of a discontinuity when $\dot{x}$ =0. Since most applications in small or medium scale fluid-power applications do not require the level of position and velocity precision at the microscopic level offered by such advanced friction models, several alternatives are available for use, three of which are applied in the following sections.

For each of the following friction models, the equations are developed and then applied to the single-platform actuator simulation in Simulink. Two cases are viewed. The first is an open loop step input that alternately sends a signal of 2.5 or 7.5 volts to the valve at a rate of 0.7 Hz, which should cause the cylinder to extend to the position limit. From this input, the response to an open-loop step response is observed. For good results, it is expected that the simulated position will closely resemble the measured position, at least maintaining the same velocity, if not the same position. Additionally, the simulated pressure should peak at the same time as the measured pressure (representing the point where stiction is overcome) and should maintain a roughly constant set of differential pressures thereafter. The second case is a closed-loop sine wave of amplitude 0.01 m about an offset of 0.02 m at a speed of 1 rad/s. This closed-loop signal, controlled by a PID controller that is identical in the measured and simulated test setups, represents the changing joint position required in joint or gait motions. A good response is indicated by similar position tracking, and a step like position and pressure curve -- the result of the ratio of static to kinetic friction. This step like motion is evident to the observer on the physical test setup, and should therefore be reflected in the simulation.

Coulomb and Coulomb-Viscous Friction Models

One of the simplest friction models is a basic Coulomb Friction model, characterized by the equation

$$F_{friction} = \begin{cases} F_C sign(\dot{x}) & if \ |\dot{x}| > 0 \\ F_{Cyl} & if \ \dot{x} = 0 \ and \ F_{Cyl} < F_C \end{cases} \quad (6)$$

where F_{Cyl} is the net force applied to the cylinder piston, and F_C is the Coulomb sliding friction force. In the system defined here (Figure 6),

$$F_C = F_{Cyl} + mg \quad (7)$$

and the Coulomb sliding friction force is defined by the coefficient of friction μ and the normal force N to be

$$F_C = \mu N \quad (8)$$

Since this model, often referred to as dry friction, does not account for the viscous component of friction, a different model that combines Coulomb and viscous forces is often applied[9], resulting in a model similar to a simplified Stribeck Curve in form, as seen Figure 7b. Assuming a constant normal force, N, this can be defined as

$$F_{stiction} = \begin{cases} F_{Cyl} & \dot{x} = 0 \ and \ |F_{Cyl}| < F_S \\ F_S - F_{Cyl} & \dot{x} = 0 \ and \ |F_{Cyl}| > F_S \\ F_C sign(\dot{x}) - C_V \dot{x} & |\dot{x}| > 0 \end{cases} \quad (9)$$

where the maximum stiction force, F_S, the Coulomb force, F_C, and the coefficient of viscous friction, C_V are determined experimentally, as done in Shu & Bone[9].

This approach was applied to the cylinder model, resulting in the behavior shown in Figure 8.

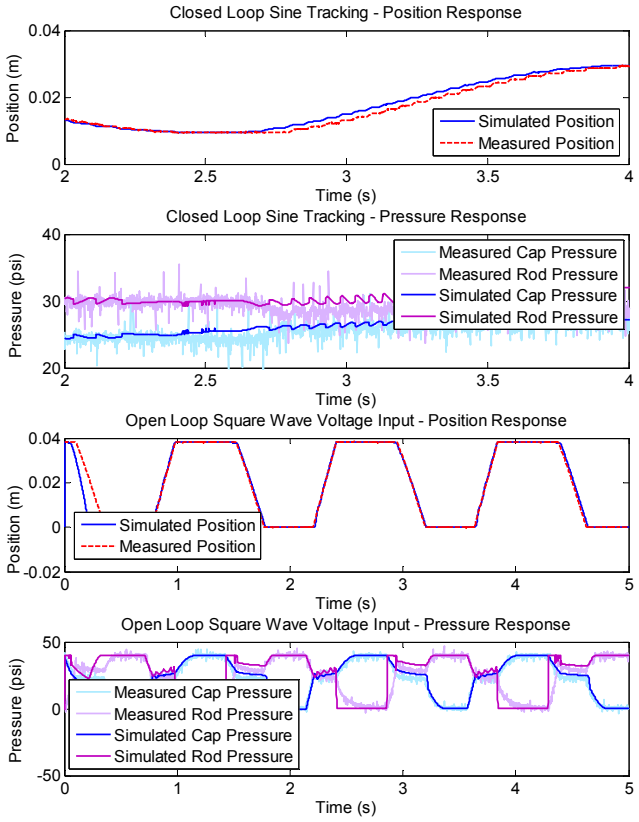

Figure 8 – Actuator Simulation with Coulomb-Viscous Friction Model

It can be seen from the responses above that the application of this model in the single-platform actuator simulation demonstrates a close correlation to the measured behavior. The closed loop sine tracking exhibits the characteristic step-like behavior and the difference between measured and simulated positions for the open loop step response is practically zero.

While this model provides an effective and simple way of obtaining relatively accurate friction models, it is largely limited in its practical implementation. Like the Stribeck and LuGre models, this friction model is characterized by a discontinuity at $\dot{x} = 0$. Accordingly, it is necessary to know all the forces acting on the system at each time step. While these forces were known for the closed form system model used in the Simulink model, they are difficult to obtain from larger scale simulation packages such as SrLib. Indeed, doing the added calculations to obtain them would likely be so computationally intensive as to effectively defeat the original purpose of using the readily available simulation package. Additionally, the discontinuity contributes toward further nonlinearity of the model and makes it more difficult to design controllers for the system.

Viscous Friction Model

A simple and frequently employed alternative[7,8] is to approximate friction with a single velocity dependent term (Figure 7c):

$$F_{Friction} = C_V \dot{x} \quad (9)$$

where C_V is the coefficient of viscous friction, determined empirically. This friction model was implemented in the simulation and produced the results depicted in Figure 9.

As can be seen, both the simulated pressure and position behavior resemble the measured behaviors. However, the correlation between measured and simulated behavior is less accurate than that visible with the more advanced model in Figure 8, particularly in pressure correlation and position behavior of the closed-loop system, where the simulated data does not exhibit the characteristic step-like increments representative of an accurate friction model.

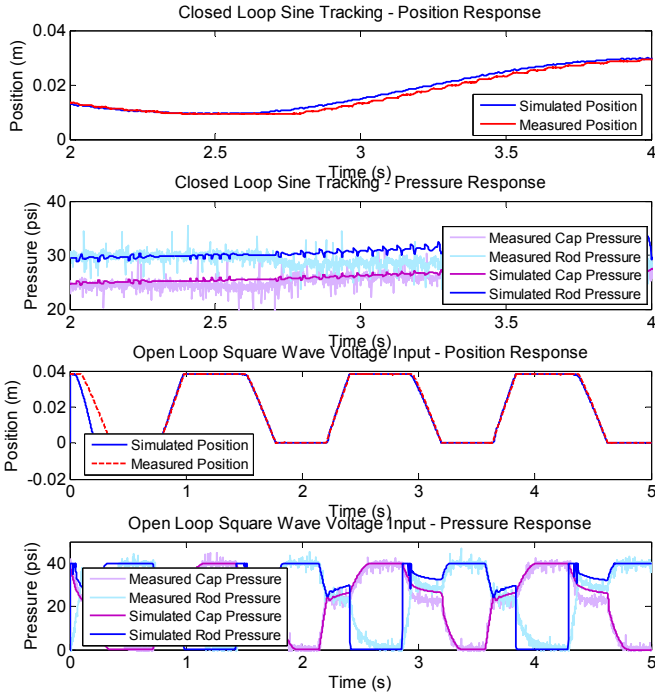

Figure 9 - Actuator Simulation with Viscous Friction Model

Continuous Coulomb-Viscous Friction Model

To avoid the discontinuity incurred by more realistic friction models while still obtaining more accurate behavior than a sole viscous friction model can provide, a friction model that approximates the stiction region with a continuous segment is applied. Literature demonstrates several techniques for approximating this region[7], such as through the use of a scaled tanh function, or by substituting a steep, saturated viscous friction curve for regions in which the absolute value of the velocity is less than some minimum value. The latter approach is used here—that is

$$F_{stiction} = \begin{cases} C_{V1}\dot{x} & |\dot{x}| < V_{\min} \\ C_{V2}\dot{x} & |\dot{x}| < nV_{\min} \\ F_C sign(\dot{x}) - C_V \dot{x} & |\dot{x}| > 0 \end{cases}$$

$$C_{V1} = \frac{F_S}{V_{\min}} \qquad (10)$$

$$C_{V2} = \frac{(F_C sign(\dot{x}) + C_V n V_{\min}) - F_S}{(n-1)V_{\min}}$$

where V_{min} is the minimum velocity to approximate the start of motion of the piston and n is an experimentally determined decimal value greater than 1. The resulting curve, shown in Figure 7d, resembles an approximate Stribeck or Coulomb-Viscous friction curve with the discontinuity removed.

This last friction model was again implemented in the single-platform simulation, with the resulting behavior display in Figure 10.

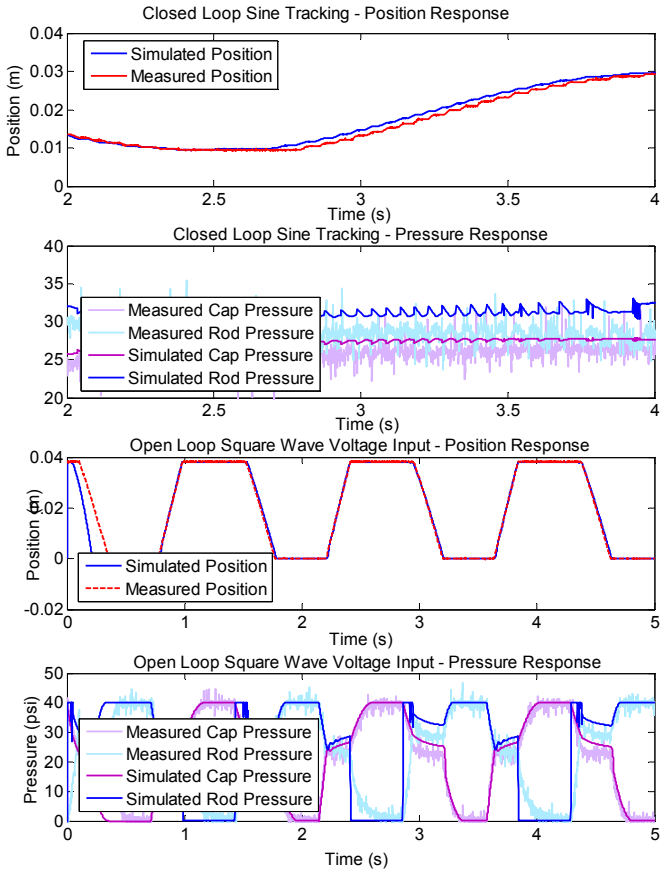

Figure 10 – Actuator Simulation with Continuous Coulomb-Viscous Friction Model

Based on these results, it is again evident that the simulated position and pressure signals in both the open and closed loop cases act favorably, demonstrating similar pressure and position behavior, and providing a response representative of an accurate friction model.

Discussion of Friction Model Variations

All three friction models used in this closed form simulation demonstrated performances that closely matched the simulated and measured pressure and position behavior. However, they are not all equally valuable for a practical simulation. As expected, the approach that uses only viscous friction (Figure 8), performs the least like the simulation, failing to exhibit the step-like position response and corresponding pressure response seen in the measured closed loop sine tracking, indicating that this friction model is not sufficient to represent the behavior of friction within the simulation.

While the Coulomb-Viscous models with and without discontinuities appear to do an equally good job of replicating cylinder pressure and position behavior based on the afore-derived results, a weakness of the continuous version is demonstrated in Figure 11. A closed loop step response sent to the actuator results in small oscillations about the set point before the system is able to settle. While these oscillations are barely noticeable from the position curve, they are evident when the velocity curve is analyzed.

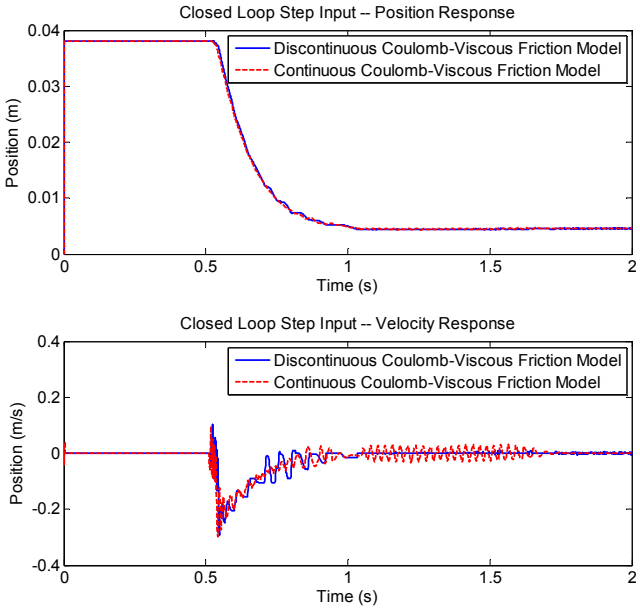

Figure 11 - CL step response for coulomb-viscous models

As previously noted, for cases necessitating a precise understanding of friction for small velocities, more advanced models can be applied and more sophisticated techniques can be used to avoid the challenge of discontinuities, yet these come at the expense of a more complex and difficult to model system. However, for the human-scale systems described here, the models discussed above provide a sufficient spectrum of available friction models for practical implementation in simulation. Even the

weakness of the continuous Coulomb-viscous friction model, shown in Figure 11, has a negligible impact on the system at hand. Because the performance of human-scale systems will rarely be severely impeded by an oscillation of less than .001 m about the set point, the models developed above clearly provide a simple and effective method for friction modeling.

Additionally, while the discontinuous Coulomb-Viscous model may be more accurate overall, additional factors are worthy of consideration. These include the linearity of the model and the ease of controller design, both of which are improved by using a continuous Coulomb-Viscous friction approximation. Taking all these factors into account, the continuous Coulomb-Viscous approximation is likely the best choice for practical implementation in an actuator simulation.

INTEGRATION WITH SRLIB

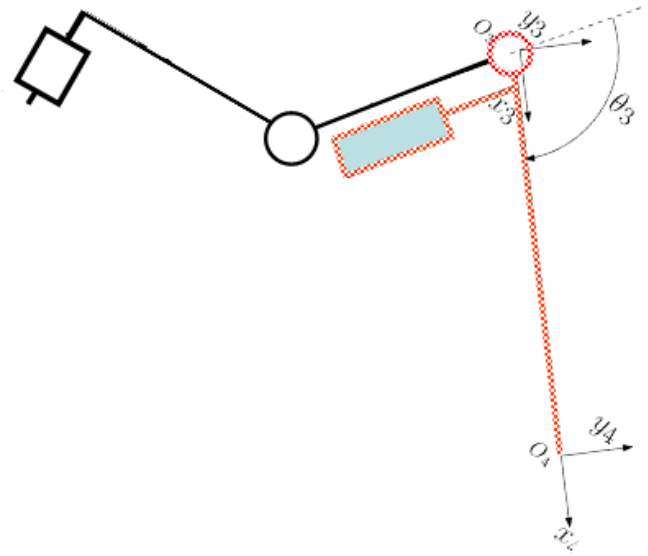

Figure 12 - Joint 3 Instantaneous geometry

The final element in providing an accurate dynamic simulation of a pneumatically actuated robot is the combination of the Simulink model with the C++ dynamics library for a complete multi-platform simulation. To do so, force outputs from the cylinder are converted to a torque based on the instantaneous geometry. To demonstrate how the overall system multi-platform simulation will perform, this configuration is applied to joint 3 of the leg, highlighted in Figure 12.

To account for friction in the joint, a rotary damping term is added to the torque output that is sent to SrLib. SrLib then calculate the dynamics and provides the Simulink model, located on a Target PC, the resulting angular position and velocity of the joint. These are converted back to stroke position and velocity and provided to the actuator model and PID controller.

Challenges

There are several key differences between this integrated model and the closed form Simulink simulation that pose challenges to smooth integration of the two dynamic simulations. These are discussed in greater detail in past publications[6].

Non Real-Time Operating Systems

While the Simulink model runs in xPC Target, a real-time system, SrLib does not, instead running on a Windows machine. The potential danger presented by this setup is that performing other tasks, such as running multiple programs, can adversely affect the performance of the dynamic simulation. To avoid such issues, the minimum number of programs is loaded on the host computer when SrLib is running.

Effect of Rendering

SrLib provides the user with a graphic presentation of the motions experienced by the dynamic model. This output is achieved by rendering an updated image of the model/terrain interaction every *n* number of time steps, where *n* is specified with SrLib. Each time a frame is rendered in the dynamic simulation, all other operations are paused for the duration of the render, resulting in pauses of up to 20 ms. Given a standard 20 fps render rate, this can cause the actuator model to fail entirely due to false velocity and position data. For the purpose of testing here, the simulation is set to render once every 10000 steps, so that these effects are effectively negligible. While this change limits the value of the simulation from a graphic perspective, haptic feedback is still enabled. Future changes to the simulation architecture, such as threading of SrLib, could also be applied to eliminate or at least reduce the impact of this issue.

Time Delay

Even without considering the impact from non real-time operating systems and rendering effects, time delay may still play a factor in the success of the overall simulation. Because torques must be sent from the target computer to SrLib on the host, processed, and then sent back again, there is a resulting delay, found to be 4 ms. This delay could impact the actuator model accuracy and would also reduce the value of a friction approximation that models the effects of stiction as a velocity dependency.

Tests

Using the methods described above, the actuator simulation was integrated with SrLib and provided with several test behaviors that would indicate performance representative of behaviors needed for gait motion. Specifically, a square wave was provided to simulate position and pressure correspondence to a sequence of

open loop step inputs, and a fast closed loop sine wave was provided to demonstrate ability to follow a changing curve, indicative of motions required for effective gait and manipulation. Both tests were applied only to the last leg joint, joint 3, which is labeled in Figure 12.

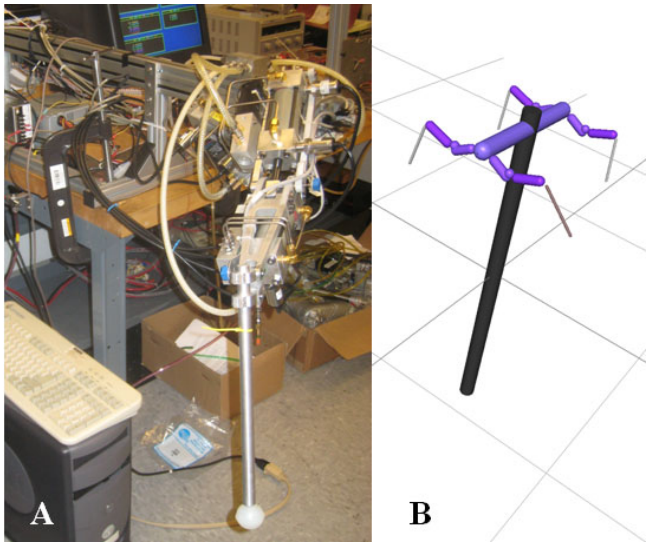

Figure 13 – (A) Actuated Leg of the Two-legged Physical Prototype used for SrLib Simulation Validation and (B) Equivalent Simulated Model

The simulated data was verified against experimental data collected from the two legged physical fixed testbed shown in Figure 13a. To represent the fixed nature of the physical prototype, the simulated model was firmly fixed to the ground by a pedestal welded through the spine, shown in Figure 13b.

Results and Discussion

Based on the observed behavior, displayed in Figure 14, the pressure acts appropriately for the desired open loop actions. However, the magnitude and duration of the steps is not as accurate as was witnessed in the closed form Simulink actuator model. Additionally, the closed loop simulated data differs greatly from the measured values, failing to demonstrate any of the characteristic peaks seen in the measured closed loop pressure response, which represent stiction forces experiences by the cylinder. This indicates that some of the challenges discussed earlier did indeed impede the performance of the total simulation.

The likely primary cause of this error is the time delay resulting from the combination of two platforms for development of this practical simulation. As noted in the "Challenges" portion of this paper discussed previously, even when there are no adverse effects from frame rendering or non-real time operating system limitations, there is still the 4 ms period required for data to complete the platform loop. That is, when a force is first output to the SrLib dynamic simulation, it takes at least 4 ms for the resulting velocity to be accounted for within the actuator model. Because of this delay, pressure and velocity, which are inherently related by equation (3), are not in sync. This would have a particularly negative effect on the modeling of stiction, which has been shown to be calculated based on the current velocity of the systems. Thus, the reduction of realism with respect to friction in the dynamic simulation following expansion to a multi-platform version is really an anticipated result of multi-platform interaction. Overall, however, the system still displays model dynamics characteristic of a pneumatically actuated system.

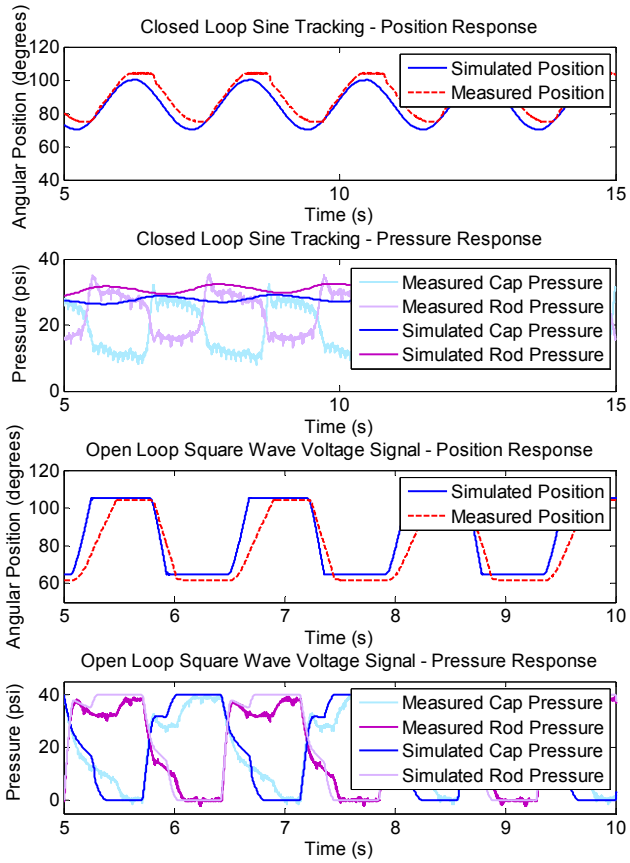

Figure 14 – Closed and open loop position and pressure behavior for a pneumatic actuator model integrated with SrLib that uses a continuous Coulomb-Viscous friction model

The results of the same tests applied to the model using the viscous friction model are shown in Figure 15. It is again evident that while the pressure and position also behave in the desired fashion for the open loop case, the magnitude is not entirely accurate. Additionally, it can be observed that attempts to compensate by adding damping (increasing the viscous friction coefficient) quickly result in an unstable system. Thus, despite the fact that while neither friction model is able to depict the level of accuracy displayed on the single-platform simulation, it is evident that a more accurate friction model is still highly desirable for a more flexible and more accurate system.

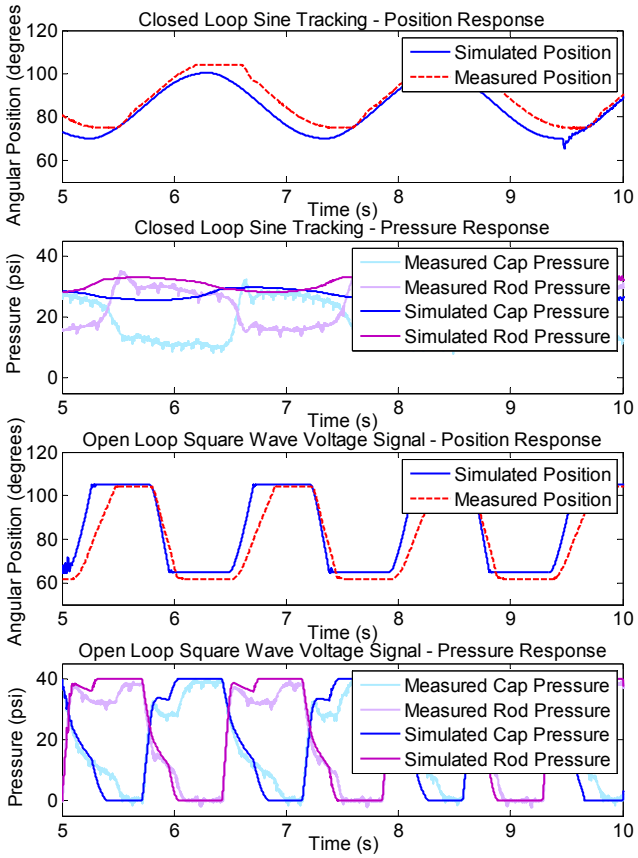

Figure 15 - Closed and open loop position and pressure behavior for a pneumatic actuator model integrated with SrLib that uses a Viscous friction model

FUTURE WORK

The results demonstrated in this paper point to the difficulty of interfacing separate, well-functioning systems. Potential improvements to the performance could be achieved through changes in the dynamic simulation architecture, such as threading the send, receive, dynamics calculation, and rendering processes. Additionally, the model could be improved upon by replacing the torque conversion with linear actuators that directly represent the behavior of the pneumatic cylinders.

The main hindrance to the realization of an accurate multi-platform simulation was found to be the time delay that inherently results from communication between the two platforms. Future work should be most directly focused on reducing the effects of this time delay. This could be achieved, for example, by developing local, low-dimensional velocity model in the Simulink software that runs in parallel with the pneumatic actuator model. Such a model would be used to anticipate changes in velocity and compensate for the lack of synchronization between pressure and velocity at points critical to accurate friction modeling.

In addition to improving performance through the changes noted above, actuator models will be provided to each joint, and inputs will be received from the Phantom Joysticks. The outputs will be sent back to the user to provide haptic feedback that reflects the effects of pneumatic actuation on the robot performance.

CONCLUSION

In this paper, the multi-platform dynamic simulation of a pneumatically actuated robot using available simulation packages combined with analytically developed actuator models is outlined, developed, and tested. Several friction models are discussed, noting that a continuous model is easier to program and more flexible to work with and design controllers for than a discontinuous model. Implementation of the various friction models in a closed-form simulation in Simulink demonstrate realistic pressure and position behavior among all three models, though they differ in their overall value. It is found that in a simple actuator simulation for a human-scale platform where precise knowledge of friction at very small velocities is not a necessity, a continuous Coulomb-Viscous friction approximation generally provides a good balance of practicality and realism. However, for cases where a more precision on a microscopic level is desired, discontinuous models, such as Stribeck curves or approximations thereof may be more appropriate.

The second portion of this paper examines the impacts of combining these actuator models with a dynamics package representative of a spectrum of available packages. Challenges, such as operating system constraints and time delay, are discussed, and the system is implemented and verified against experimental data. Performance results indicate that while the actuator provides the appropriate behavior to the model, the scale is skewed, indicating adverse effects on model integrity as a result of interfacing the two models. Both friction models are examined, and it is shown that the Coulomb-Viscous model still shows considerably better behavior and stability than the viscous friction approximation.

The current performance of the model reflects actual pneumatic actuator behavior, as demonstrated by the open and closed loop pressure behaviors. Since the primary purpose of the simulation is to guide design changes to the operator interface and controllers rather than simulate exact behavior, the performance demonstrated here provides a sufficient result for future work.

Overall, it can be shown that accurate friction modeling is an important component of achieving good accuracy for a cylinder model. However, as the result is expanded and implemented in more versatile available simulation tools such as SrLib, many potential challenges damage the integrity of the model. Accordingly, an advanced multi-component simulation that combines existing tools (rather than being constructed as one complete closed-form simulation), will inherently reduce the level of

simulation accuracy and reduce the overall realism. Thus, unless it is possible to develop local models to predict velocity and compensate for the lack of synchronization between friction and pressure, placing substantial effort into precise modeling of friction components is likely a wasted effort. Indeed, it is probably more effective for the user to combine a generalized model with a simulation library for a final product that reflects the characteristic behavior, if not the exact motions, of the actual system.

ACKNOWLEDGMENTS

The authors would like to thank JD Huggins and Michael Valente for their assistance with hardware and software, as well as Seoul National University's Robotics Lab for the development and assistance with SrLib. This research has been supported by the CCEFP, and has benefited from collaborators at Vanderbilt University and North Carolina Agriculture and Technological University.

REFERENCES

1) Schneider, D., *Robin Murphy Roboticist to the Rescue.* Spectrum, IEEE, 2009. 46(2): p. 36-37
2) Driewer, F., H. Baier, and K. Schilling, "Robot-human rescue teams: a user requirements analysis," Advanced Robotics, Vol. 19, 2006, p. 819-838.
3) Song, S-M and Waldron, K., Machines that Walk: the adaptive suspension vehicle, MIT Press series in artificial intelligence, Cambridge, Mass, 1989.
4) Sangyoon, L. and Kim, G.J., "Effects of haptic feedback, stereoscopy, and image resolution on performance and the presence in remote navigation." International Journal of Human-Computer Studies, Vol. 66, 2008, pp 701-717.
5) Gentry, S., Wall, S., Oakley, I., and Murray-Smith, R., "Got rhythm? Haptic-only lead and follow dancing," Proc. Eurohaptics Conference, Dublin, 2003, pp. 481-488.
6) Book, W., Daepp, H., Kim, T. and Radecki, P., "An interactive simulation for a fluid-powered legged search and rescue robot," Proceedings of 2010 International Symposium on Flexible Automation, Tokyo, July 2010.
7) Andersson, S., Soderberg, A., and Bjorklund, S., "Friction models for sliding dry, boundary and mixed lubricated contacts," Tribology International, Vol. 40, No. 4, April 2007, pp. 580-587.
8) Al-Dakkan, K.A., Barth, E.J., and Goldfarb, M., "Dynamic constraint-based energy-saving control of pneumatic servo systems," Transactions of the ASME Journal of Dynamic Systems, Measurement and Control, Vol. 128, 2006, pp. 655-662.
9) Shu, N. and Bone, G.M., "Development of a nonlinear dynamic model for a servo pneumatic positioning system," Mechatronics and Automation, IEEE, Vol. 1, 2005, pp. 43-48.
10) Thomas, M.B and Maul, G.P., "Considerations on a mass-based system representation of a pneumatic cylinder," Journal of Fluids Engineering, Transactions of the ASME, Vol. 131, April 2009, pp. 041101-7 – 041101-10.
11) Hong, I.T and Tessmann, R.K., "The dynamic analysis of pneumatic systems using HyPneu," Proceedings of the National Conference on Fluid Power, National Fluid Power Association, Vol. 47, 1996, pp. 61-70.

DEFINITIONS, ACRONYMS, ABBREVIATIONS

A	Area	m^2
C_1	Constant 1	
C_2	Constant 2	
C_d	Discharge coefficient	0.2
CoG	Center of Gravity	
DoF	Degrees of Freedom	
F	Force exerted by actuator	N
F_C	Coulomb sliding Force	N
F_{Cyl}	Net force applied to the cylinder piston	N
$F_{friction}$	Friction force	N
F_S	Maximum Stiction Force	N
P	Pressure	Pa
R	Universal gas constant (air)	287 J/kg K
T	Instantaneous internal cylinder temperature	ºK
b	Viscous damping coefficient	kg/s
k	Ratio of specific heats (air)	1.4
m	Mass of piston and load	kg
M	Total mass of piston and mounted load	kg
$\dot{m}$	Mass flow rate	kg/m^3
n	Constant decimal value greater than 1	
N	Normal force	N
$x, \dot{x}, \ddot{x}$	Actuator position, velocity, acceleration	m,m/s,m^2/s
$\theta_1, \theta_2, \theta_3$	Rotation angles of robot leg for joints 1,2, and 3, respectively	degrees
μ	Coefficient of sliding friction	
V_{min}	Minimum velocity required to approximate the start of motion of the piston	,/s

Subscripts

atm	Atmospheric
c	cap-side
d	downstream
r	Rod-side
O	Orifice
u	upstream